Irradiation Hardening and Microstructure Characterization of Zr -1% Nb During Low Dose Neutron Irradiation

Carolina Vazquez[1,2*], Eugenia Zelaya[3,4], Ana María Fortis[1,2], Patricia B. Bozzano[1,2]

1. Gerencia de Materiales, Centro Atómico Constituyentes, Av. General Paz 1499 (1650) San Martín, Buenos Aires, Argentina
2. Instituto Sabato-UNSAM/CNEA, Av. General Paz 1499 (1650) San Martín, Buenos Aires, Argentina
3. División Física de Metales - CNEA e Instituto Balseiro (UNCuyo), Av. Bustillo km 9.5, 8400 S.C. de Bariloche, Argentina
4. Consejo Nacional de Investigaciones Científicas y Técnicas (CONICET), Godoy Cruz 2290, CABA, Argentina
E-mail: cvazquez@cnea.gov.ar

Abstract: Due to low neutron absorption cross section, high mechanical strength, high thermal conductivity and good corrosion resistance in water and steam, Zirconium alloys are widely used as fuel cladding material in nuclear reactors. During life-time of a reactor the microstructure of this alloy is affected due to, among other factors, radiation damage and hydrogen damage. In this work mechanical properties changes on neutron irradiated Zr-1wt.% Nb at low temperatures (< 100 °C) and low dose (3.5×10^{23} n m^{-2} (E > 1 MeV)) were correlated with hydrides and crystal defects evolution during irradiation. To achieve this propose, tensile tests of: 1) Non-hydrided and non-irradiated material, 2) Hydrided and non-irradiated material and 3) Hydrided and irradiated material were performed at 25 °C and 300 °C. Different phases, hydrides and second phase precipitates were characterized by transmission electron microscopy (TEM) techniques. For the hydrided and irradiated material, the ductility decreased sharply with respect to the hydrided and non-irradiated material, among other factors, due to the change in the microstructure produced mainly by neutron irradiation. Even if the presence of the hydride ζ (zeta) was observed, both in the irradiated and non-irradiated material, tensile tests showed that ζ-hydrides did not affect ductility, since hydrided samples are more ductile than non-hydrided samples.
Keywords: Zirconium alloys; Radiation damage; Hydrogen; Electron microscopy; Tensile tests.

1. Introduction

Zirconium alloys are commonly used as structural material of components in nuclear industry, due to their excellent properties such as low thermal neutron absorption cross section, corrosion, and creep resistances in pressure environments at reactor operating temperatures [1-3].

One of the effects of irradiation which mostly affects mechanical behavior is irradiation hardening. Since fast neutron irradiation leads to growth of dislocation loops, hardening, loss of ductility, growth, and creep. [4-8], it is very important to determine the degree of embrittlement of irradiated components. In addition, it is necessary to establish how radiation affects the phases present in the precipitated material during and after irradiation [9].

Another effect to consider is that produced by hydrogen (H). When Zr-based alloys are used in PWR (pressurized water reactors) or PHWR (pressurized heavy water reactors) H is released as a by-product of the hydrolytic reaction between cooling water and Zr. When hydrogen is absorbed into the Zr matrix and exceeds its solid solubility at reactor temperature, zirconium hydrides precipitate in the matrix, affecting physical and mechanical properties of the alloy. These effects have been extensively studied in the last years [10, 11] including the embrittlement due to hydride-assisted cracking [12,13].

Several Zirconium-1% niobium alloys have been used as material for fuel cladding, pressure tubes in PWR and in Russian pressurized water reactors (VVER) [7,8, 10]. Mostly used Zr-1% Nb alloys are: M5 (Zr-1% Nb-0.05% Fe), E110 (Zr-1% Nb-0.01% Fe), E635 (Zr-1.2 Sn-1.0 Nb -0.35 Fe), ZIRLO (Zr-1% Nb-1% Sn-0.1 Fe), HANA6 (Zr-1.0 Nb-0.5 Cu), N18 (Zr-1.0 Sn-0.3 Nb-0.3 Fe-0.1 Cr), N36 (Zr-1.0 Sn-1.0 Nb-0.3 Fe) [2, 14].

In Zr-1wt.% Nb alloys, different phases are present depending on the chemical composition and the thermomechanical history. The most reported phases are: (hexagonal compact structure) α-Zr, (both body-centered cubic) β-Zr, β-Nb and the ternary phases Zr-Nb-Fe [6]. Hydrides can be formed as stable δ ($ZrH_{1.5+x}$) and ε (ZrH_2) phases, and the metastable γ (ZrH) and ζ (Zr_2H), the latter currently considered as a fourth phase. The ζ phase is potentially important for the formation and growth of more stable δ and ε hydrides [15].

Under irradiation, all these phases undergo microstructural and microchemical modifications that could affect their in-service performance [16-18]. Thus, there is interest to analyse the behavior of Zr-1wt% Nb alloy in a radioactive environment that combines ζ hydride's nucleation, hydrogen in solution and defects created by irradiation [19].

In this work, the interaction between hydrides, second phase particles and radiation at 25 ℃ y 300 ℃ in Zr-1wt.% Nb has been analyzed. A group of samples of this material was hydrided and irradiated in the CNEA-RA3 nuclear reactor. They were placed in a capsule located in one of the reactor irradiations channels. The neutron fluence was 3.5×10^{23} n m^{-2} after an irradiation of 30 days. Microstructural analysis was performed by transmission electron microscopy techniques.

2. Experimental procedure

Materials were provided by the company Teledyne Wah Chang Albany, as 1 mm thickness straps. The straps were rolled in order to obtain a final thickness of 0.5 mm. Tensile test specimens were then prepared by cutting with a numerical control machine down to a size small enough in order to minimize the dose of activity after irradiation.

The alloy composition can be observed in Table 1.

Table 1. The chemical composition of zirconium alloys matrix in units of weight percent (wt%) quantitatively given by the manufacturer of the alloy.

Zr-1wt.% Nb	Nb	C	Fe	O	Cr
Nominal Composition (wt.%)	1	0.0014	0.05	0.084	0.0074

All specimens were annealed at 450 ℃ for 24 h and distributed in three groups:
1) non-hydrided and non-irradiated material
2) hydrided non-irradiated material
3) hydrided and irradiated material

The samples were hydrided with a gaseous charge of 200 ppm of hydrogen, using a Sievert device at 350 ℃. They were subsequently annealed for three days in argon atmosphere at 380 ℃.

One of the batches of hydrided samples was irradiated at room temperature in the CNEA-RA3 nuclear reactor. The neutron fluence was 3.5×10^{23} n m^{-2} (E > 1 MeV) after an irradiation of 30 days.

In all groups, tensile tests were carried out at 25 ℃ and 300 ℃. Thin sheets were obtained from the heads of each specimen for their microstructural characterization.

Tensile tests were performed in an Instron machine with a maximum load cell of 50 kN, using an inverted traction system. Ad-hoc clamps were designed for the assemblage of irradiated specimens to minimize the manipulation of irradiated material.

All the tensile tests were performed at the same nominal crosshead speed of 0.2 mm min^{-1}, being the strain rate 1.5×10^{-4} s^{-1}.

Wedge shape specimens for electron microscopy were mechanically polished down to a thickness of 0.2 mm. Discs 3 mm in diameter were punched out and mounted in a polishing device. The disks were then electropolished in a Struers Tenupol 5 twin jet electropolisher using an electrolyte of 90% ethanol and 10% perchloric acid at -30 ℃ and 18 V.

Wedge shape thin films thus obtained allowed to study the hydrides in different planes of α-Zr matrix. TEM images were obtained in a Philips CM200, operated at 160 kV, and high-resolution images in a FEI TECNAI G2 operated at 200 kV.

The simulation image was obtained using a JEMS software [20].

3. Results

TEM micrograph of the starting material (non-rolled strip) is shown in Figure 1 [21]. Figure 2 shows the micrograph of the 50% laminated material that was cut with a numerical control machine and subjected to a relieving stress heat treatment at 450 °C for 24 hours.

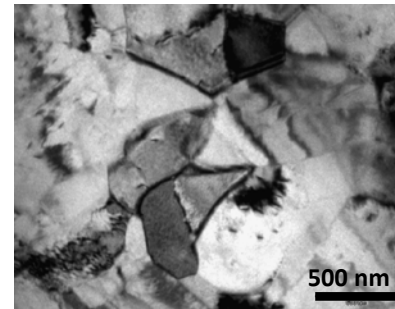**Figure 1.** TEM bright field image of the as-received material showing the α-Zr matrix.

Figure 2. TEM bright field image after the lamination and the thermal treatment (24h at 450 ºC) showing α-Zr matrix.

3.1. Mechanical properties

Uniaxial tensile tests were performed on Zr-1%Nb at room temperature and at the reactor operation temperature (~300 °C), see Figure 3 a) and b).

The change in ultimate tensile strength (UTS), yield strength (YS), total elongation (ε_{tot}) and uniform elongation (ε_{unif}) values were extracted from the stress-strain curves, see Table 2.
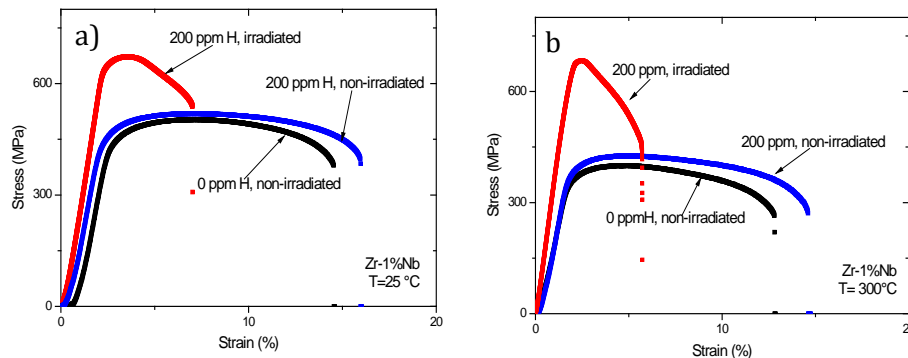

Figure 3. a) Stress-strain curves at 25 ºC, b) Stress-strain curves at 300 ºC

Table 2. Results of the tensile tests of Zr-1wt.% Nb samples

Batch	Test temperature ºC	YS MPa	UTS MPa	ε_{unif} %	ε_{tot} %
1	25	389	503	5.20	13.00
Non-hydrided-Non-irradiated	300	323	400	2.64	11.635
2	25	395	519	5.84	14.42
Hydrided-Non-irradiated	300	345	427	3.51	13.46
3	25	584	673	1.56	5.36
Hydrided-Irradiated	300	460	684	0.66	4.52

3.1.1 Non-irradiated material

When comparing the curves corresponding to hydrided and non-hydrided specimens, it was found that at room temperature there is no noticeable effect on hardening (YS and UTS vary approximately 2%), Fig. 3a). Total elongation due to the presence of this type of hydrides was 10 % (see Table 2). On the other hand, when performing the same comparison with the tensile tests carried out at 300 ºC, it can be seen an increase of 6% in yield stress and ultimate strength, due to the presence of those hydrides Fig. 3b). Furthermore, the total elongation increased because the hydrides improve the total elongation by 10%. This phenomenon has been observed more clearly at 300 °C.

3.1.2 Irradiated material

After low-temperature (<100 ºC) neutron irradiation at 3.5×10^{23} n m^{-2} (E > 1 MeV), the samples showed an increase of 67% (at 25 °C) and 75% (at 300 °C) in UTS and YS as compared to the case of hydrided and non-irradiated material. Simultaneously, a drastic decrease in ductility is observed at both temperatures (Figure 3a), b)), of around 35%, in ε_{tot} showing the relevance of the radiation effects on mechanical properties.

3.2 Microstructure of material

3.2.1 Non-irradiated material

The microstructural analysis of the first group, i.e., non-hydrided and non-irradiated, shows the typical α-Zr phase with equiaxial grains (see Figure 4 (a)). Spherical precipitates of the phase β-Zr were observed randomly distributed throughout the matrix. This phase is body centered cubic (BCC) with lattice parameter a = 0.3568 nm [17]. The average size of these precipitates was 199 nm with a dispersion of +/- 10 nm (Figure 4 (b)).

ζ (zeta) hydrides were observed for the hydrided samples. They were characterized as a needle-shaped HCP structure, with lattice parameters a = 0.33 nm and c = 1.029 nm, corresponding to a trigonal crystal with spatial group P3m1. In general, they were in planes [0 0 1] of the α-Zr matrix [22]. The average length of these hydrides was 186 nm with a dispersion of +/- 10 nm (see Figure 5 (a), (b), (c)).
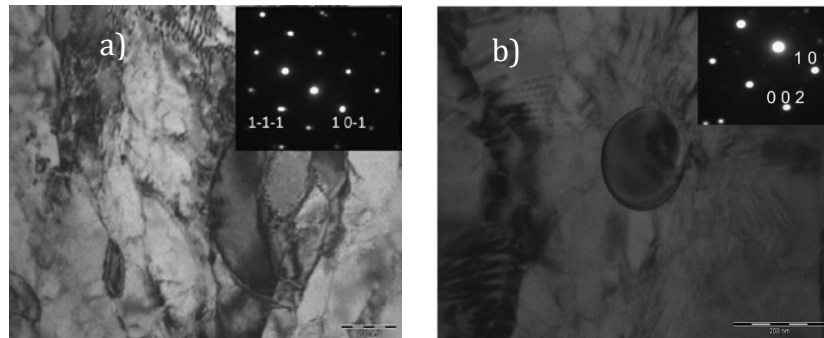

Figure 4. Non-hydrided / non-irradiated samples, (a) TEM bright field image showing α-Zr matrix and the corresponding SAED pattern, [1 0 1] zone axis, (b) TEM bright field image of β-Zr precipitate phase in a α-Zr matrix and the SAED pattern of the precipitate, [0 1 0] zone axis.
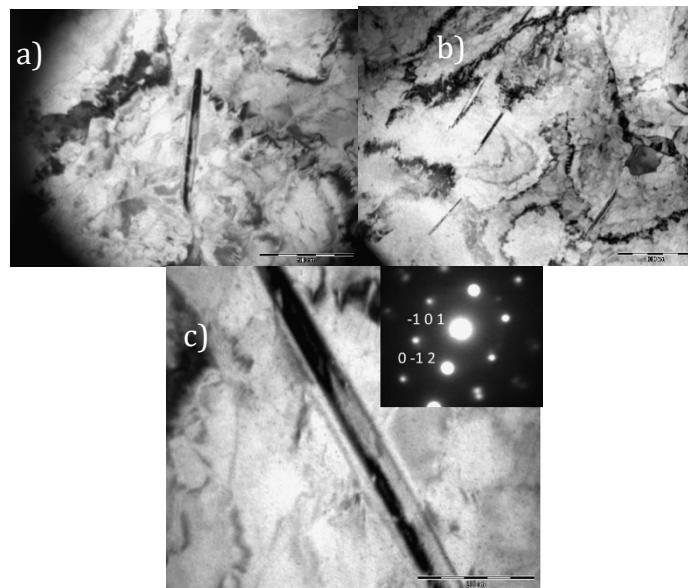

Figure 5. Hydrided/non-irradiated samples, (a) and (b) TEM bright field image of ζ-hydrides in the α-Zr matrix, (c) enlarged images of ζ-hydrides and SAED pattern of ζ-hydrides, [1 0 -1] zone axis.

3.2.2 Irradiated material

Regarding hydrided and irradiated specimens, small precipitates of Zr (Nb, Fe)$_2$ were identified. These precipitates are known to be hexagonal compact structure (HCP), with spacial group symmetry P63/mmc and lattice parameters a = 0.5335 nm and c = 0.866 nm [2, 23]. Due to their small size this phase was identified by electron diffraction patterns. The superposition of the matrix accounts for the uncertainty of the data that give compositional values higher than those corresponding to a Laves phase [14]. However, when observing high resolution images and its respective simulation, (Figure 6a) and b)), it is confirmed that the contrast obtained is consistent with the presence of a crystalline structure of the precipitated corresponds to a Laves phase known as C14-structure type MgZn$_2$ [2].

The presence of these precipitates was observed surrounding the ζ-hydrides at the above-mentioned irradiation dose (see Figure 7(a)).

The metastable hexagonal ω-Zr phase was identified, distributed randomly in the α-Zr matrix. This phase has spatial group symmetry P6/mmm and lattice parameters a = 0.5034 nm and c = 0.3124 nm. The mean size of these precipitate was measured as 7 nm with a dispersion of +/- 1 nm. Due to their small size (see Figure 8) this phase was identified as such by electron diffraction.
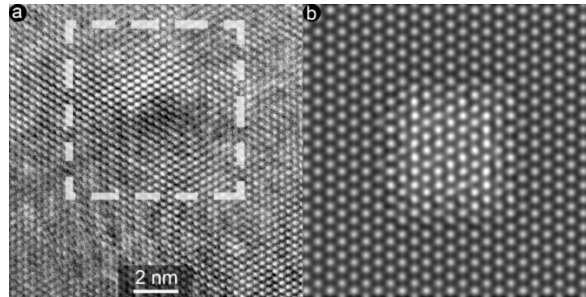

Figure 6. a) High resolution image of matrix and Zr (Nb Fe)$_2$ precipitate, and b) simulation of the area inside the while dash lines of α-Zr matrix, and a precipitate with crystalline structure C14.The defocus was 100 nm and the sample thickness was 5.1 nm.
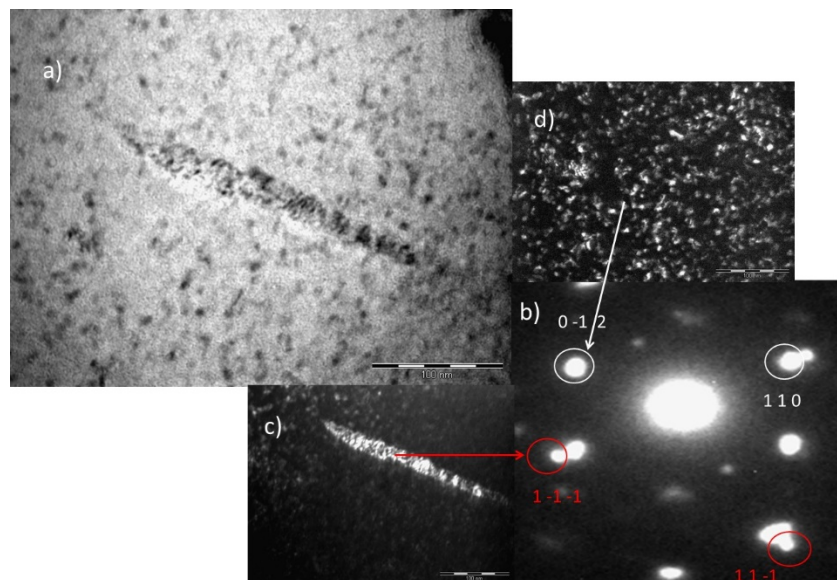

Figure 7. (a) TEM bright field image of ζ-hydrides and Zr (Nb, Fe)$_2$ precipitates in hydrided and irradiated Zr-1wt.% Nb sample. b) the SAED pattern of the image a), c) TEM dark field image of ζ-hydrides, [1 0 1] zone axis. The red arrow shows the spots corresponding to this hydride, d) TEM dark field image of Zr(Nb, Fe)$_2$ precipitates, [2 -2 -1] zone axis. The white arrow shows the spot which corresponds to this precipitate.
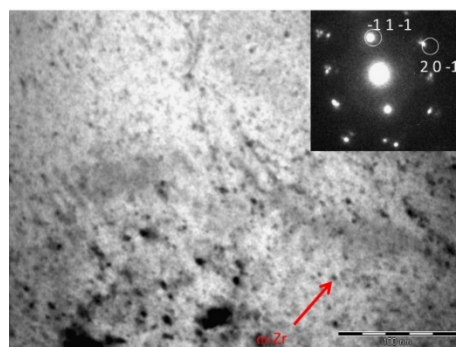

Figure 8. TEM bright field image of ω-Zr phase in hydrided and irradiated Zr-1wt.% Nb sample and the corresponding SAED pattern, [1 3 2] zone axis.

4. Discussion

4.1. Non-irradiated material

When analyzing the stress-strain curves behavior of the hydrided and non-hydrided specimens (see Figure 3), it was observed that at room temperature the presence of hydrides did not generated an increase in hardening nor ductility. Instead at 300 °C a slight increase can be seen in hardening, and ductility seems too slightly improve.

This anomalous behavior could be attributed, among other factors, to the type of hydride and its possible location. In this work, a type of hydride known as ζ-hydride was found, see Figure 5. This hydride was characterized by Zhao et.al (2008) [22] in Zircaloy-4. It is needle-shaped with HCP structure, corresponding to a trigonal crystal with space group P3m1[22, 24]. Also, by studies carried out by Thuinet et.al (2012), it was oberved that ζ-hydrides nucleated more easily than γ-hydrides because they have a lower interfacial energy [25]. According to the cooling rate, the ζ-hydrides transform to give rise to metastable γ-hydrides.

Another aspect which should be considered is the hydride orientation in the matrix. In this work, the texture of laminated sample favors hydrides to be located in certain planes. Zhao proposed that a new phase may play an important role in the stress-reorientation of hydrides. [1] since the hydride orientation is determined by the nucleation process and is maintained constant during growth. In presence of external stresses, elastic interaction between the precipitation-induced strain and the applied stress may have an influence on the orientation of the hydrides [26-29]. In addition, Zhu and coworkers completed a study on the ductility of each zirconium hydrides. Their research indicated that ζ-hydrides and γ-hydrides are more ductile than the α-Zr matrix [1, 30]. The observed stress-strain curves behavior, in this study, could be explained as the sum of these factors.

It is also necessary to consider the microstructure of this alloy, especially the presence of β-Nb precipitates [31], as a result of the heat treatments carried out. Dislocation pile-ups at these precipitates are believed to play an important role in work hardening [32]. However, the amount of precipitated phase does not seem to be significantly.

4.2. Irradiated material

In the stress-strain curves of hydrided and irradiated material it was observed a large increase of ultimate tensile strengths (UTS) and a considerable decrease in the total elongation with respect to the non-irradiated samples. This indicates that the behavior of the mechanical properties of the irradiated and hydrided material is opposite to those corresponding to non-irradiated and hydrided samples.

The irradiated samples were analyzed by transmission electron microscopy (TEM). The presence of the same hydrides as in the previous case was observed, as well as microstructural changes resulting from radiation damage [33].

One of the microstructural changes that have been noted is the presence of second-phase precipitated particles (SPP), around the ζ-hydrides. The incipient precipitation has been crystallographically characterized by two different techniques, HRTEM and SAD, as Laves-C14 phases. Due to of the small size of the precipitates observed in the present work, was not possible to determine their composition.

At present, determining the composition of these precipitates is of great interest. The Laves-C14 phases have strict stoichiometries AB_2. However, the compositional designation of Zr $(Nb, Fe)_2$ has a very wide range [34]. Studying the interaction between these precipitates and hydrides is of vital importance to understand how it would affect the mechanical properties of this alloy. Idress et al. [35] demonstrated that irradiation induces the Fe dissolution, and this dissolved Fe was found in the form of spherical precipitates in the α-Zr matrix [35]. As an H atom is smaller than a Fe atom, it moves more easily occupying the interstitial sites of the cells delaying the Fe atoms movement in the α-Zr matrix [36].

Another possibility was proposed by Burr and coworkers [36], who studied the effects of SPP on the H absorption of Zr alloys [36- 38]. Their results have showed that these particles could potentially be used as H sinks by decreasing the H availability for hydriding. However, under irradiation, Fe atoms spread out of the SPP faster than other elements [38-40]. Then, in the case of Nb-containing Laves phases, it would increase the affinity of residual SPP for H, suggesting that H will likely segregate to them, thus depleting the H content in the Zirconium metal, this phenomenon is limited to low doses (3.5×10^{23} n m^{-2}) [36].

The presence of the ω phase has also been observed due to decomposition of the β-Zr phase induced by radiation (see Figure 8) [41].

In the present work, it was not possible to observe the presence of dislocation loops. The first loops to nucleate at low temperatures and low doses (5×10^{25} n m^{-2}) are type-$\langle a \rangle$ loops, varying from 5 to 20 nm in size [42]. Also, Cockeram et al. [43, 44] have reported that $\langle a \rangle$ and $\langle c \rangle$ -type dislocation loops as well as groups of point defects can only be observed if the neutron irradiation fluence is greater than 0.058×10^{24} n m^{-2}. If dislocation loops were present, then they were below the size detection limit for the TEM (nominally ≤ 0.4 nm). It could also be expected to find these loops lying on the prism planes {1 0 $\bar{1}$ 0} or {1 1 $\bar{2}$ 0} [45], although recent studies

suggested that most ⟨a⟩-type dislocation loops do not perfectly lie on these prism planes but tilt a little towards the basal planes [46]. These were not the planes that were analyzed in this work (see Figure 3a)).

In Figure 9 the ductility of hydrided and irradiated and non-irradiated alloy is compared at 25 °C and 300 °C.
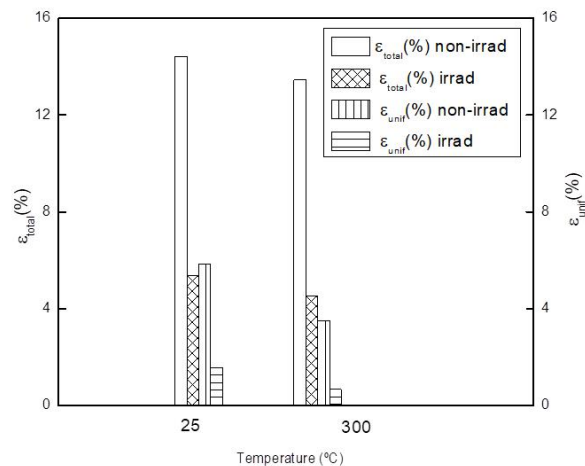

Figure 9. Comparison of the ductility of hydrided and irradiated and non-irradiated Zr-1%Nb at 25 °C and 300 °C.

It is observed that the total elongation of the irradiated and non-irradiated material varies by approximately 60% at both temperatures, however the difference in non-uniform elongation between the irradiated and non-irradiated material is greater at 300 °C.

Mechanical property degradations of the irradiated specimens may be attributed to the ζ-hydrides orientation produced during the nucleation process and by the radiation damage in matrix. The presence of radiation generated loops, Zr (Nb, Fe)$_2$ precipitates and ω-phase produce microstructural changes at the nano scale, which could explain the decrease in mechanical properties such as a sharp increase in ultimate tensile strength. The irradiation produced defects represent barriers to the movement of dislocations so that the radiation hardening is based upon the interaction of mobile dislocations with the irradiation produced defects.

It can be concluded that, at the present dose (3.5×10^{23} n m^{-2} (E > 1 MeV)), the microstructural changes generated by radiation are the most responsible for the damage, as measured through the mechanical stress changes, rather than that produced by ζ-hydrides.

5. Conclusions

Mechanical tests and microstructure studies of Zr-1wt.% Nb hydrided with 200 ppm of hydrogen and non-irradiated and irradiated were carried out at 25 ℃ and 300 ℃.

The presence of the metastable ζ-hydride was observed in both cases. However, tensile behavior is different. In the case of hydrided and non-irradiated, no significant change in hardening and ductility were noted at room temperature. Instead at 300 ℃ a slight increase can be seen in ductility of the hydrided alloy. This anomalous behavior could be attributed to the type of hydride and its possible orientation in the matrix.

In the mechanical tests of hydrided and irradiated Zr-1wt.% Nb, a great decrease in the ductility and great increase in hardening were observed at both temperatures. The mechanical properties behavior suggested a reordering of ζ-hydride and the presence of the microstructural changes due to the radiation damage acting according to the scattered barrier model.

Acknowledgments

6. References

[1] Bair J, Zaeem MA, Tonks M. A review on hydride precipitation in Zirconium alloys. Journal of Nuclear Materials. 2015; 466: 12-20. https://doi.org/10.1016/j.jnucmat.2015.07.014

[2] Liang J, Zhang M, Ouyang Y, Yuan G, Zhu J, Shen J, Daymond M R. Contribution on the phase equilibria in Zr-Nb-Fe system. Journal of Nuclear Materials. 2015;466: 627-633. https://doi.org/10.1016/j.jnucmat.2015.09.005

[3] Topping M, Harte A, Ungar T, Race CP, Dumbill S, Frankel P, Preuss M. The effect of irradiation temperature on damage structures in proton-irradiated Zirconium alloys. Journal of Nuclear Materials.2019; 514: 358-367. https://doi.org/10.1016/j.jnucmat.2018.12.006

[4] Yu H, Yao Z, Idress Y, Zhang HK, Kirk MA, Daymond MR. Accumulation of dislocation loops in the αphase of Zr Excel alloy under heavy ion irradiation. Journal of Nuclear Materials. 2017; 491: 232-241. https://doi.org/10.1016/j.jnucmat.2017.04.038

[5] Nordlung K, Zinkle S, Sand A, Granberg HF, Averback R, Stoller R, Suzudo T, Malerba L, Banhart F, Weber W, Willaime F, Dudarev SL, Simeone D. Primary radiation damage: A review of current understanding and models. Journal of Nuclear Materials. 2018; 512: 450-479. https://doi.org/10.1016/j.jnucmat.2018.10.027

[6] Grossbeck ML, Mazias PJ, Rowcliffe AJ. Modeling of strengthening mechanisms in irradiated fusion reactor first wall alloys. Journal of Nuclear Materials. 1992; 191-194(B): 808-812. https://doi.org/10.1016/0022-3115(92)90584-8

[7] Pokor C, Averty X, Brèchet Y, Dubuisson P, Massoud JP. Effect of irradiation defects on the work hardening behavior. Scripta Materialia. 2004; 50 (5): 597– 600. https://doi.org/10.1016/j.scriptamat.2003.11.029

[8] Dong Q, Yao HZ, Daymond MR. Irradiation damage and hardening in pure Zr and Zr-Nb alloys at 573 K from self-ion irradiation. Materials and Design. 2019; 161: 147-159. https://doi.org/10.1016/j.matdes.2018.11.017

[9] Vazquez C, Fortis AM, Bozzano P. Comparison of Mechanical Properties of Zr-1%Nb and Zr-2.5%Nb Alloys. In: International Congress of Science and Technology of Metallurgy and Materials, SAM-CONAMET 2013. Puerto Iguazu. Argentina. August 20-23. 2013. Procedia Materials Science. 2015; 8: 478-485. https://doi.org/10.1016/j.mspro.2015.04.099

[10] Ells CF. Hydride precipitates in Zirconium alloys (A review). Journal of Nuclear Materials. 1968; 28: 129-151. https://doi.org/10.1016/0022-3115(68)90021-4

[11] Huang JH, Huang SP. Effect of hydrogen contents on the mechanical properties of Zircaloy-4. Journal of Nuclear Materials. 1994; 208 (1-2): 166-179. https://doi.org/10.1016/0022-3115(94)90208-9

[12] Kaplar E, Yegorova L, Lioutov K, Konobeyev A, Jouravkova N, Smimov V, Goryachev A, Prokhorov V, Makarov O, Yeremin S, Svyatkin A. International Agreement Report: Mechanical Properties of Un irradiated and Irradiated Zr-1% Nb Cladding. U.S. Nuclear Regulatory Commission Washington DC. 2001.

[13] Garat V, Denble D, Dunn B, Mardon JP. Quantification of the margins provided by M5 cladding in accidental condition. In: 2012 Top Fuel Reactor Fuel Performance. Manchester. United Kingdom. September 2-6.2012. Top Fuel 2012 Transient Fuel Behaviour. European Nuclear Society. Brussels. Belgium. 2012

[14] Harte A, Griffiths M, Preuss M. The characterization of second phases in the Zr-Nb and Zr-Nb-Sn-Fe alloys: A critical review. Journal of Nuclear Materials. 2018; 505: 227-239. https://doi.org/10.1016/j.jnucmat.2018.03.030

[15] Bair J, Zaeem MA, Schwen D. Formation path of δ hydrides in zirconium by multiphase field modeling. Acta Materialia. 2017; 123: 235-244. https://doi.org/10.1016/j.actamat.2016.10.056

[16] Doriot S, Onimus F, Gilbon D, Mardon J-P, Bourlier F. Transmission electron microscopy study of second phase particles irradiated by 2MeV protons al 350°C in Zr alloys. Journal of Nuclear Materials. 2017; 494: 398-410. https://doi.org/10.1016/j.jnucmat.2017.07.020

[17] Adrych-Brunning A, Gilbert MR, Sublet J-Ch, Harte A, Race CP. Modelling the interaction of primary irradiation damage and precipitates: Implications for experimental irradiation of zirconium alloys. Journal of Nuclear Materials. 2018; 498: 282-298. https://doi.org/10.1016/.j.jnucmat.2017.10.022

[18] Francis E, Babu RP, Harte A, Martin TL, Frankel P, Jadernas D, Romero J, Hallstadius L, Bagot PAJ, Moody MP, Preuss M. Effect of Nb and Fe on damage evolution in a Zr-alloy during proton and neutron irradiation. Acta Materialia. 2019; 165: 603-614. https://doi.org/10.1016/j.actamat.2018.12.021

[19] Khatamian D. Solubility and partitioning of hydrogen in metastable Zr-based alloys used in the nuclear industry. Journal of Alloys and Compounds. 1999; 293-295: 893-899. https://doi.org/10.1016.S0925-8388(99)00388-6

[20] JEMS Electron Microscopy Software Jave Version: 48431U2019b04. Stadelmann, 2014-2019. JEMS-SWISS.

[21] Fortis AM, Vazquez CA. Mechanical Test and Microstructure Characterization of Hydride Zr-1wt%Nb. In: 11th International Congress on Metallurgy & Materials SAM/CONAMET 2011. Rosario, Argentina. October 18-21. 2011. Procedia Materials Science. 2012; 1: 520-527.https://doi.org/10.1016/j.mspro.2012.06.070

[22] Zhao Z, Morniroli JP, Legris A, Ambard A, Khin Y, Legras L, Blat-Yrieix M. Identification and characterization of a new zirconium hydride. Journal of Microscopy. 2008; 232 (3): 410-421. https://doi.org/10.1111/j.1365-2818.2008.02136

[23] Granovsky MS, Cannay M, Lena E, Arias D. Experimental investigation of the Zr corner of the ternary Zr-Nb-Fe phase diagram. Journal of Nuclear Material. 2002; 302: 1-8. https://doi.org/10.1016/S0022-3115(02)00718-3

[24] Zhao Z, Blat-Yrieix M, Morniroli J-P, Legris A, Thuinet L, Kihn Y, Ambarrd A, Legras L. Characterization of Zirconium Hydrides and Phase Field Approach to a Mesoscopic-Scale Modeling of Their Precipitation. In: *Zirconium in the Nuclear Industry: 15th International Symposium*. June 24-27.2007. Oregon. USA. STP 1505 Zirconium in the Nuclear Industry; 15th International Symposium. West Conshohocken, PA; Journal of ASTM International; 2009; 5: 29-50. https://doi.org/10.1520/JAl101161

[25] Thuinet L, Besson R. Ab initio study of competitive hydride formation in zirconium alloys. Intermetallics. 2012; 20 (1): 24-32. https://doi.org/10.1016/j.intemet.2011.08.005

[26] Thuinet L, De Backer A, Legris A. Phase-field modeling of precipitate evolution dynamics in elastically inhomogeneous low-symmetry systems: Application to hydride precipitation in Zr. Acta Materialia. 2012; 60 (13-14): 5311-5321. https://doi.org/10.1016/j.actamat.2012.05.041

[27] Thuinet L, Legris A. Elastically driven morphology of coherent trigonal precipitates inside a close-packed hexagonal matrix. Acta Materialia. 2010; 58 (6): 2250-2261. https://doi.org/10.1016/j.actamat.2009.12.012

[28] Thuinet L, Legris A, Zhang L, Ambard A. Mesoscale modeling of coherent zirconium hydride precipitation under an applied stress. Journal of Nuclear Materials. 2013; 438: 32-40. https://doi.org/10.1016/j.jnucmat.2013.02.034

[29] Zhang Y, Bai Y-M, Yu J, Tonks MR, Noordhoek MJ, Phillpot SR. Homogeneous hydride formation path in α-Zr: Molecular dynamics simulations with the charge-optimized many-body potencial. Acta Materialia. 2016; 111: 357-365. https://doi.org/10.1016/j.actamat.2016.03.079

[30] Zhu W, Wang R, Shu G, Wu P, Xiao H. First-Principles Study of Different Polymorphs of Crystalline Zirconium Hydride. Journal Physical Chemistry C.2010; 114: 22361-22368. https://doi.org/10.1021/jp109185n

[31] Motta A, Capolungo L, Chen L, Cinbiz MN, Daymond MR, Koss DA, Lacroix E, Pastore G, Simon P-C, Tonks MR, Wirth BD, Zikry MA. Hydrogen in zirconium alloys: A review. Journal of Nuclear Materials. 2019; 518: 440-460. https://doi.org/10.1016/j.jnucmat.2019.02.042

[32] Jang K-N, Kim K-T. The effect of neutron irradiation on hydride reorientation and mechanical property degradation of zirconium alloy cladding. Nuclear Engineering and Technology. 2017; 49 (7): 1472-1482. https://doi.org/10.1016/j.net.2017.05.006

[33] Gurovich BA, Frolov AS, Kuleshova EA, Maltsev DA, Safonov DV, Alekseeva EV. TEM-studies of the dislocation loops and niobium-based precipitates in E110 alloy after operation in VVer-type reactor conditions. Materials Characterization. 2019; 150: 22-30. https://doi.org/10.1016/j.matchar.2019.01.014

[34] Ramos C, Saragovi C, Granovsky M, Arias D. Effects of Nb content on the Zr_2Fe in intermetallic stability. Journal of Nuclear Materials. 2003; 312 (2-3): 266-269. https://doi.org/10.1016/S0022-3115(02)01677-X

[35] Idress Y, Yao Z, Cui J, Shek GK, Daymond MR. Zirconium hydrides and Fe redistribution in Zr-2.5%Nb alloy under ion irradiation. Journal of Nuclear Materials. 2016; 480: 332-343. https://doi.org/10.1016/j.jnucmat.2016.08.031

[36] Burr PA, Murphy ST, Lumley SC, Wenman MR, Grimes RW. Hydrogen solubility in zirconium intermetallic second phase particles. Journal of Nuclear Materials. 2013; 443 (1-3): 502-506. https://doi.org/10.1016/j.jnucmat.2013.07.060

[37] Burr PA, Murphy ST, Lumley SC, Wenman MR, Grimes RW. Hydrogen accommodation in Zr second phase particles: Implications for H pick-up and hydriding of Zircaloy-2 and Zircaloy-4. Corrosion Science. 2013; 69: 1-4. https://doi.org/10.1016/j.corsci.2012.11.036

[38] Yang W, Tucker R, Cheng B, Adamson R. Precipitates in zircaloy: Identification and the effects of irradiation and thermal treatment. Journal of Nuclear Materials. 1986; 138 (2-3): 185-195. https://doi.org/10.1016/0022-3115(86)90005-X

[39] Griffiths M, Gilbert R, Carpenter G. Phase instability, decomposition and redistribution of intermetallic precipitates in Zircaloy-2 and -4 during neutron irradiation. Journal of Nuclear Materials. 1987; 50 (1): 53-66 https://doi.org/10.1016/0022-3115(87)90093-6

[40] Long F, Griffiths M, Yao Z, Daymond MR. Characterization of phases in the Zr-Nb-Fe ternary system at the Zr-Nb rich side of the phase diagram. Journal of Nuclear Materials. 2020; 534: 152142. https://doi.org/10.1016/j.jnucmat.2020.152142

[41] Yu H, Dong Q, Yao Z, Zhang HK, Kirk MA, Daymond MR. In-situ study of heavy ion irradiation induced lattice defects and phase instability in β-Zr of a Zr-Nb alloy. Journal of Nuclear Materials. 2019; 522: 192-199. https://doi.org/10.1016/j.jnucmat.2019.05.028

[42] Idress Y, Zao Z, Sattari M, Kirk MA, Daymond MR. Irradiation induced microstructural changes in Zr-Excel alloy. Journal of Nuclear Materials. 2013; 441 (1-3): 138-151. https://doi.org/10.1016/j.jnucmat.2013.05.036

[43] Cockeram BV, Smith RW, Leonard KJ, Byun TS, Snead LL, Development of microstructure and irradiation hardening of Zircaloy during low dose neutron irradiations' at nominally 358°C. Journal of Nuclear Materials. 2011; 418 (1-3): 46-61. https://doi.org/10.1016/j.jmucmat.2011.07.006

[44] Saini S, Gayathri N, Sharma SK, Devi A, Srivastava AP, Neogy S, Mukherjee P, Pujari PK. Microstructural investigation of irradiation damage behavior of proton irradiated Zr-1wt.%Nb cladding alloy. Journal of Nuclear Materials. 2020; 528: 151894. https://doi.org/10.1016/j.jnucmat.2019.151894

[45] Konings RJM. Comprehensive Nuclear Materials. Chapter 4.01. Elsevier. Amsterdam. 2012. https:// doi.org/ 10.1016/B978-0-08-056033-5.00064-1.

[46] Dai C, Balogh L, Yao Z, Daymond MR. The habit plane of $< a >$ -type dislocation loops in α-zirconium: an atomistic study. Philosophical Magazine. 2017; 97 (12): 1-13. https://doi.org/10.1080/14786435. 2017.1287441